KTH Electrical Engineering

Cascaded Converters with Gate-Commutated Thyristors

Experimental Verification and Auxiliary Power Supply

TOMAS MODEER

Doctoral Thesis
Stockholm, Sweden 2015

TRITA-EE 2015:021
ISSN 1653-5146
ISBN 978-91-7595-581-0

KTH School of Electrical Engineering
SE-100 44 Stockholm
SWEDEN

Akademisk avhandling som med tillstånd av Kungl Tekniska högskolan framlägges till offentlig granskning för avläggande av teknologie doktorsexamen Måndagen den 8:e Juni 2015 klockan 10.15 i Kollegiesalen, Kungl Tekniska Högskolan, Brinellvägen 8, Stockholm.

© Tomas Modeer, April 2015

Tryck: Universitetsservice US AB

Abstract

This thesis describes an effort to investigate the use of gate-commutated thyristors (GCTs) in cascaded converters. Cascaded converters, such as modular multilevel converters (M2Cs) and cascaded H-bridge converters (CHBs), have proved to be especially suitable in high-voltage, high-power applications. All of the most important advantages of cascaded converters, e.g. redundancy and scalability, can be attributed to the modular structure. Of special interest regarding the choice of semiconductor power devices is the reduced requirement on the switching frequency of individual devices. This brings a shift in the trade-off between switching and conduction losses, where the latter has more importance in cascaded converters than in other topologies. This shift favors thyristor-type devices like the GCT, which can achieve very low conduction losses.

To quantify the potential gain in the application of GCTs in cascaded converters the losses have been calculated and a comparison between different submodule implementations has been presented. The comparison has shown that GCTs can provide 20-30% lower losses compared to insulated-gate bipolar transistors (IGBTs) in a typical HVDC application. In order to verify the low losses of GCT-based submodules, extensive work has been put into building and testing full-scale submodules employing GCTs. A resonant test circuit has been developed in which the submodules can be tested in steady-state operation which allows calorimetric measurements of the losses. The calorimetric measurements have verified that the loss calculation was reasonable and not lacking any important components.

A drawback of GCTs is that the gate-drive units require much more power than gate-drive units for comparable IGBTs. In order to employ GCTs in high-voltage cascaded converters some means of supplying this power in the submodule must be provided. One option is to take this power from the submodule dc-link, but this requires a dc-dc converter capable of high input voltages. A tapped-inductor buck converter with a novel, autonomous high-side valve was developed for this application. The autonomous operation of the high-side valve allows reliable operation without galvanic isolation components. A converter with a high-side valve with series-connected MOSFETs capable of an input voltage of 3 kV has been presented.

Sammanfattning

Denna avhandling beskriver arbete som syftat till att undersöka möjligheten att använda gate-kommuterade tyristorer (gate-commutated thyristors, GCT) i kaskad-kopplade omvandlare. Kaskad-kopplade omvandlare, t.ex. i modulära multi-nivå omvandlare (modular multilevel converter, M2C) och kaskad-kopplade H-bryggor (cascaded H-bridge, CHB), har visat sig särskilt lämpade för tillämpningar med hög effekt och spänning. Denna typ av omvandlare har en mängd fördelar, såsom redundans och skalbarhet, som beror av dess modulära struktur. Av särskilt intresse vad gäller valet av halvledare är ett minskat behov av kommuteringar hos de enskilda ventilerna. Detta ger en förskjutning i balansen mellan kommuterings- och led-förluster, där de senare har större vikt i kaskadkopplade omvandlare än i andra omvandlare. Detta gynnar halvledarventiler av tyristor-typ såsom GCTer, eftersom dessa kan ge väldigt låga ledförluster.

För att kvantifiera hur stor förlustbesparing GCTer kan ge i kaskad-kopplade omvandlare har en förlustberäkning utförts och en jämförelse mellan olika submodulkonstruktioner presenterats. Jämförelsen har visat att GCTer kan ge 20-30 % lägre förluster än IGBTer i en typisk HVDC-tillämpning. För att verifiera att så verkligen är fallet, har mycket av arbetet fokuserat på att bygga submoduler med GCTer i fullskala samt att utveckla en testkrets för att kunna testa submodulerna i fortvarighet. Kalorimetriska mätningar på denna testkrets har visat att de förlustberäkningar som utförts är riktiga och att inga förlustkomponenter av större vikt har utelämnats.

En nackdel med GCTer är att gate-drivdonen kräver mer effekt än gate-drivdon för IGBTer i motsvarande effektklass. För att kunna använda GCTer i kaskadkopplade omvandlare måste något sätt att tillhandahålla denna effekt lokalt i submodulen ordnas. En tapped-inductor dc-dc-omvandlare med en ny, autonom, ventilkonstruktion har utvecklats för detta ändamål. Detta ger en tillförlitlig omvandlare utan behov av komponenter för galvanisk isolation.

Acknowledgment

This thesis concludes the work I have carried out at the Department of Electrical Energy Conversion, KTH Royal Institute of Technology since May 2010. First of all I would like to thank my supervisors Hans-Peter Nee and Staffan Norrga for their kind guidance and support during the project. I also would like to thank them for striving for an open, up-beat and forward-looking atmosphere at the department. For the nice working environment I must of course also thank all my colleagues in the department, both staff and PhD students. Many thanks to Eva Petterson and Peter Lönn for all help during the years. For the experimental work in this project I have had very much help from Jesper Freiberg in manufacturing parts and building the test setup. For this I am very grateful. I also want to thank my fellow PhD students Luca Bessegato and Matthijs Heuvelmans for inspiring collaboration on research and papers.

I would like to thank everyone at ABB who has helped me and supported us with hardware and expertise. Special thanks to Tobias Wikström who has been instrumental in everything related to GCTs during this work, including generously supplying devices for testing.

Finally, I would like to thank my family and my fiancée Marina for their endless support and encouragement.

Stockholm, May 2015
Tomas Modeer

Contents

1 Introduction **1**
- 1.1 Main Contributions of the Thesis . . . 2
- 1.2 Outline of the Thesis . . . 3
- 1.3 List of Appended Publications . . . 3
- 1.4 Related Publications . . . 5

2 Cascaded Converters **7**
- 2.1 Topologies and Applications . . . 8
- 2.2 Advantages and Characteristics of the M2C . . . 9

3 Power Semiconductors in Cascaded Converters **13**
- 3.1 Unipolar Devices . . . 14
- 3.2 Bipolar Devices . . . 15
- 3.3 Wide Band-Gap Devices . . . 17
- 3.4 Loss comparison . . . 17

4 Auxiliary Power Supplies **21**
- 4.1 Switch-mode Converters . . . 22
- 4.2 Tapped-inductor Buck Converter . . . 22
- 4.3 Series-input Parallel-output Converters . . . 24
- 4.4 Rainstick Converter . . . 25

5 Submodule Test Circuit **27**
- 5.1 Test Circuit Topologies . . . 27
- 5.2 Control Structure . . . 29
- 5.3 Calorimetric Loss Measurement . . . 30

6 Experimental Results **33**

7 Conclusions **39**
- 7.1 Future Work . . . 40

List of Acronyms **41**

List of Figures **42**

Bibliography **45**

Publication I

Publication II

Publication III

Publication IV

Publication V

Publication VI

Publication VII

Publication VIII

Chapter 1

Introduction

Worldwide the electricity grids are undergoing a fundamental change. It is not a quick and revolutionary change, but rather a gradual adaptation towards new requirements as they arise. In addition to the steady increase of transmission capacity it includes the incorporation of ever more renewable energy sources. A large part of the renewable sources, i.e. solar and wind, are of an intermittent, uncontrollable nature. Under favorable conditions such non-controllable sources may produce more power than is consumed locally, and the excess energy from these sources must be either stored or transmitted to other areas. Another option is to counteract the intermittent power production by other, controllable, energy sources such as hydro power. In order to successfully balance the fluctuations when a large fraction of the energy sources are of the intermittent nature additional measures need to be taken. Among the options are: load leveling/shedding (i.e. demand response), storage (pumped hydro, batteries), and transmission over longer distances. Arguably, to allow for more renewable energy sources to be used, all of these will need to be applied to some degree.

The first option of load shedding, which could be for example more sophisticated control of cool storage and building heating and air conditioning, can be relatively inexpensive to implement and gives rise to very little additional losses. Although some increased losses can be expected from the intermittent power use this should have a marginal effect on overall efficiency.

The second option of grid-connected storage suffers mainly from high cost per stored unit of energy and low efficiency. Pumped-hydro storage can achieve the lowest cost and is moderately efficient [1–4]. Arguably, the use of (hybrid) electric vehicle (HEV/EV) batteries is currently not very attractive as the lifetime charge/discharge cycles are better used, i.e. worth more, in vehicle propulsion. However, the charging of HEV/EV batteries lends itself well to controlled load leveling schemes. A further proposed use of HEV/EV batteries is as a source of ultra-peak power shaving. It is, however, questionable if the very low utilization can motivate the cost of integration.

The third option, transmission over longer distances, has the potential to provide a highly efficient and cost effective alternative, both by itself and as a complement to the other options. It is also a necessity in order to connect remote hydro- and wind-power to urban centra, e.g. the hydro dams in Scandinavia and the off-shore wind parks in the North Sea to the population- and industry-dense regions in central and western Europe. The most efficient means of long-range electric transmission is by high-voltage direct current (HVDC) transmission systems. Currently, most HVDC connections are point-to-point connections while only a few multi-terminal high-voltage direct current (MTDC) systems exist. There is, however, ongoing research and development on so called dc grids in which a larger number of stations would be connected in a meshed grid similar to the existing ac grids. While dc transmission has some distinct advantages, ac remains the best solution for distribution and short-haul transmission. There is, therefore, a need for ac-dc/dc-ac converter stations in both ends of an HVDC link, or in the case of MTDC, one at each terminal, to connect to the ac grids.

The converter stations can be based on either current-source converters (CSCs) or voltage-source converters (VSCs), the type having quite important implications on the system. Current-source converters are based on thyristor technology and can achieve very high efficiency, but come with some drawbacks. First, in thyristor-based line-commutated converters the current flow cannot be reversed and power reversal instead has to be achieved by changing the voltage polarity on the line. This not only precludes the use of CSCs in HVDC systems requiring cable connections, e.g. under-sea or urban installations, but also makes them unsuitable for dc grids. Further disadvantages include the inability to power a weak ac grid or re-energize an unenergized grid, i.e. there is no black-start capability.

Voltage source converters do not have the disadvantages associated with CSCs but have had lower efficiency in the past. However, the efficiency of VSC-based HVDC has improved and with the advent of new, cascaded-type converters, it is likely that the efficiency will be on par with CSC HVDC. Therefore, the development of cascaded converters is important to meet the future demands on our electrical grids. While there has been much research on the control of cascaded converters and on system level aspects, comparably little attention has been paid to the submodules. This thesis is focused on issues relating more to the individual submodules in such converters.

1.1 Main Contributions of the Thesis

The main scientific contributions of the work presented in this thesis are:

1. The use of gate-commutated thyristors (GCTs) in cascaded converters has been investigated and the possible efficiency gains have been quantified by simulations and verified by full-power experiments.

2. A dc-dc converter based on a tapped-inductor buck converter with a novel, autonomous, high-side valve suitable for use in auxiliary power supplies in submodules has been presented.

3. A resonant test circuit topology which allows for full power testing of high-power submodules under conditions similar to those in a real application, while having modest requirements on the testing hardware, has been developed.

1.2 Outline of the Thesis

Chapter 2 describes the modular structure of cascaded converters together with a brief overview of their distinct advantages and disadvantages and the new challenges in designing such converters.

Chapter 3 gives an overview of available semiconductor switch devices suitable for use in cascaded converters. The achievable efficiency gains by using thyristor-type devices is discussed.

Chapter 4 discusses the need for supplying gate unit power in the submodules from the main circuit and different alternatives are discussed. Also a solution based on a tapped-inductor buck converter is presented.

Chapter 5 discusses the need for full-power testing of converter submodules, alternative test setups, and finally presents a resonant test circuit suitable for testing high-power submodules.

Chapter 6 presents the setup and results from the testing of two 1 MVA GCT-based submodules in the proposed resonant test-circuit.

1.3 List of Appended Publications

I. **T. Modeer**, H.-P. Nee, and S. Norrga, "Loss Comparison of Different Sub-Module Implementations for Modular Multilevel Converters in HVDC Applications," in *Proc. European Conf. Power Electronics and Applications EPE*, pp. 1–10, 2011.

The first publication presents a loss comparison between submodules based on IGBTs and IGCTs. Half-bridge as well as full-bridge and clamped-double submodules are considered. A nominal frequency concept is introduced to simplify comparison of dissimilar semiconductor devices and allow pre-selection of suitable candidates. The losses are calculated over a large number of fine-grained time-steps and a thermal model is used to solve for the device temperatures. It is shown that the use of IGCTs can reduce the submodule losses considerably for all submodule topologies. In the half-bridge case the IGCT alternative offers approximately 20% lower losses compared to the IGBT alternative.

II. **T. Modeer**, H.-P. Nee, and S. Norrga, "Loss Comparison of Different Sub-Module Implementations for Modular Multilevel Converters in HVDC Applications," in *EPE Journal: European Power Electronics and Drives Journal*, vol. 22, no. 3, pp. 32–38, 2012.

The second publication extends on Publication I and includes experimental verification of the loss calculation method used.

III. **T. Modeer**, S. Norrga, and H.-P. Nee, "High-Voltage Tapped-Inductor Buck Converter Auxiliary Power Supply for Cascaded Converter Submodules," in *Proc. Energy Conversion Cong. Expo. (ECCE)*, pp. 19–25, 2012.

The third publication presents the tapped-inductor buck converter with a novel, autonomous, high-side valve. The converter has an input voltage rating of 3 kV which makes is suitable for use in an auxiliary power supply in cascaded converter submodules utilizing 4.5 kV IGCTs.

IV. **T. Modeer**, M. Zdanowski, and H.-P. Nee, "Design and Evaluation of Tapped Inductors for High-Voltage Auxiliary Power Supplies for Modular Multilevel Converters," in *Proc. International Power Electronics and Motion Control Conference (EPE-PEMC 2012 ECCE Europe. IEEE)*, 2012.

The fourth publication describes the design and testing of tapped inductors combining high voltage isolation and low leakage making them suitable for use in a converter such as described in Publication III.

V. L. Bessegato, **T. Modeer**, and S. Norrga, "Modeling and Control of a Tapped-Inductor Buck Converter with Pulse Frequency Modulation," in *Proc. Energy Conversion Cong. Expo. (ECCE)*, 2014.

The fifth publication presents a viable pulse frequency modulation control of the tapped-inductor buck converter presented in Publication III. It also describes a thyristor-based start-up circuit which allows for reliable starting of the converter without any additional power rail.

VI. **T. Modeer**, S. Norrga, and H.-P. Nee, "High-Voltage Tapped-Inductor Buck Converter Utilizing an Autonomous High-Side Switch," in *IEEE Transactions on Industrial Electronics*, vol. 62, no. 5, pp. 2868–2878, 2015.

The sixth publication extends on Publication III with improved voltage sharing between the devices in the high-side valve, higher efficiency, and a more detailed description of the converter operation.

VII. **T. Modeer**, S. Norrga, and H.-P. Nee, "Resonant Test Circuit for High-Power Cascaded Converter Submodules," in *Proc. European Conf. Power Electronics and Applications*, pp. 1–10, 8–10 Sep. 2013.

The seventh publication presents a resonant test circuit topology which allows for steady-state testing of high-voltage, high-power cascaded submodules. With this type of resonant circuit a low harmonic current waveform can be achieved even at very low switching frequencies. The circuit further has the benefit of modest demands on testing hardware in addition to two submodules. In addition, the apparent power requirement on the power source for the testing is very low and also the short-circuit power is very small.

VIII. **T. Modeer**, and S. Norrga, and H.-P. Nee, "Implementation and Testing of High-Power IGCT-based Cascaded-Converter Cells," in *Proc. Energy Conversion Congress and Exposition (ECCE)*, 2014.

The eighth publication presents the design of IGCT-based submodules and the testing of the submodules in the resonant test circuit described in Publication VII.

1.4 Related Publications

- M. Heuvelmans, **T. Modeer**, and S. Norrga, "Soft-switching cells for high-power converters," in *Annual Conference of the IEEE Industrial Electronics Society (IECON)*, 2014.

  This publication describes how the auxiliary resonant commutated pole (ARCP) topology could be used to build GCT-based soft-switching submodules. A loss calculation and comparison between such soft-switching submodules and conventional hard-switching submodules is presented.

Chapter 2

Cascaded Converters

Cascaded converters are a comparably new type of power electronic converters consisting of one or more strings of series-connected converter submodules. The prominent characteristics and advantages of cascaded converters are due to this series, or cascaded, structure. The submodules generally have a fairly simple internal structure, typically just containing either a half-bridge or full-bridge, a dc-link energy storage capacitor and the necessary control electronics. An example of a string and a half-bridge submodule is shown in Fig. 2.1. In each half-bridge submodule,

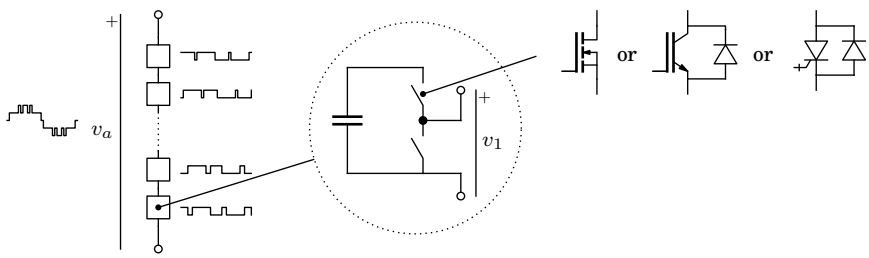

Figure 2.1: A string of submodules, the central concept of cascaded converters, showing simplified voltage waveforms of submodules and the string. Also shown is the simplified structure of a half-bridge submodule and alternative valve realizations.

there are two switches, or valves, which allow the submodule capacitor voltage to be selectively included in the string voltage. When the upper valve is conducting the capacitor voltage is added, or inserted, into the string voltage and conversely the lower valve allows bypassing of the capacitor such that its voltage is not added to the string voltage. The string voltage thus depends on the state of the submodule valves and the individual submodule capacitor voltages. As the voltage across the string is shared, i.e. divided, among the submodules while the full string current goes through all modules, this can be considered the dual of converters with parallel-connected modules, e.g. interleaved dc-dc converters.

2.1 Topologies and Applications

Two major types of cascaded converters have seen widespread use. The first, cascaded H-bridge converters (CHBs), utilize H-bridge submodules capable of bipolar output, i.e. the submodules can insert the capacitor voltage with both positive and negative polarity, and hence the strings are also capable of bipolar output voltage. Such converters have been used in static compensators (STATCOMs), shown in Fig. 2.2, since the late 1990s [5,6], which allow control of harmonics and reactive power in ac grids. By appropriate control of the converter, which amounts to controlling the

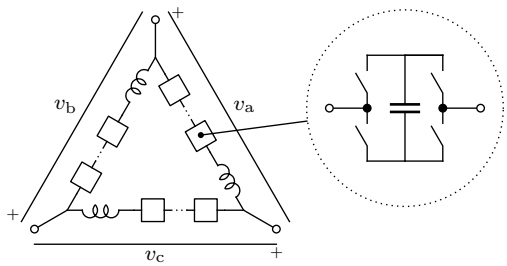

Figure 2.2: Cascaded H-bridge static synchronous compensator (STATCOM). Also shown is the simplified structure of a full-bridge submodule.

gate signals of the submodules, the power flow in and out of the submodules can be made to cancel over time and the submodule capacitor voltages can be controlled to a constant average voltage.

The second cascaded converter type that has seen widespread use is the modular multilevel converter (M2C), shown in Fig. 2.3. The M2C was first presented in 2002 [7] and has numerous advantages compared to other converter topologies, especially with regard to high voltage applications. In contrast to CHB STATCOMs, which only have an ac connection, M2Cs are used for ac-dc and dc-ac conversion. As this includes active power flow the control of the submodule capacitor voltages is somewhat different from that in a CHB STATCOM. Most importantly, in inverter operation the active power output of fundamental frequency is balanced by, mainly, a dc input power flow, both at the string level and also in the individual submodules. This balancing is the same in rectifying operation, but the power flow and the input/output nomenclature is of course reversed.

In addition to the use of M2Cs in HVDC transmission, the converters can also be used in a back-to-back configuration, as shown in Fig. 2.4, in various ac applications. Such converters can be used to interconnect ac grids with different line frequencies, grids which are not synchronized or grids with different number of phases.

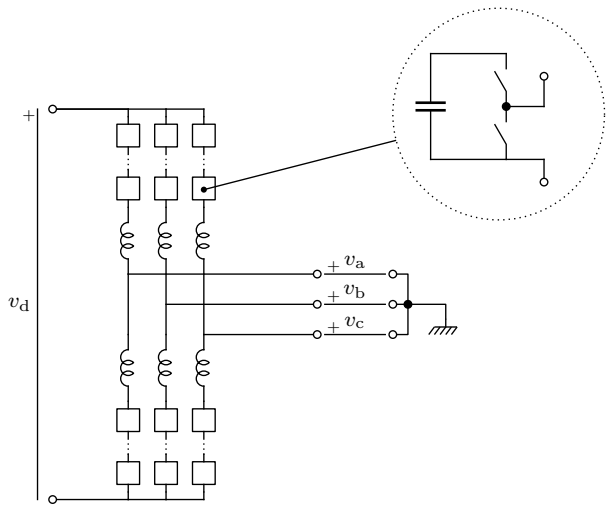

Figure 2.3: Modular multilevel converter (M2C). Also shown is a half-bridge submodule, but many other submodule topologies have been proposed.

2.2 Advantages and Characteristics of the M2C

The prominent advantages of the M2C, as stated in [7] are:

- redundancy of semiconductor devices
- low harmonic content multilevel waveform requiring very little filtering even at very low switching frequencies
- even voltage sharing: device tolerances and capacitance to ground has little impact on device voltages
- scalability: voltage and power level can be chosen "freely" while using standardized modules

These advantages are not unique to M2Cs but are in fact shared by all cascaded converters and will be discussed in some more detail in the following.

Local Commutation

As the commutation of current from one valve to the other is local to a single submodule, the switching is not greatly affected by conditions external to the submodule. These local commutation loops eliminate the need for balancing circuits and tight timing control. It also eliminates the voltage limit imposed by balancing

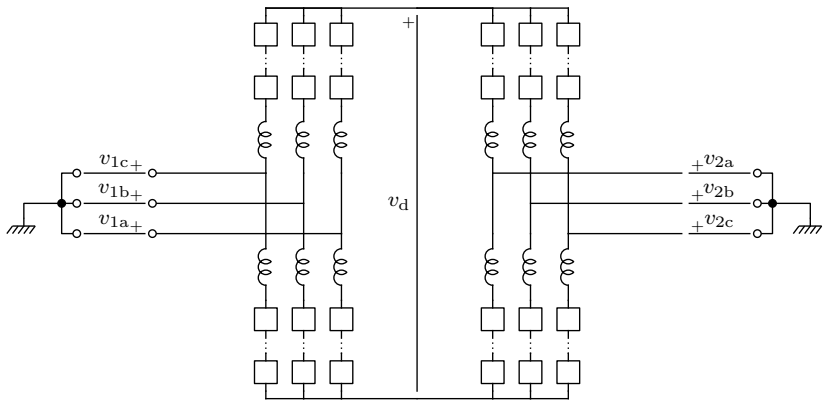

Figure 2.4: Back-to-back M2C.

of series-connected switch devices. By solving the voltage balancing problem the cascaded structure enables converters of much higher voltage and power ratings than what can be achieved by earlier two- and three-level converter topologies.

Multilevel Waveform

In a cascaded converter, the modules can be switched such that the string voltages are within less than one capacitor voltage of their reference. This means that for converters with a reasonably large number of submodules, the output voltage has very little harmonic content and little or no filtering is needed to fulfill even quite strict requirements on harmonics. This drastically reduces the need of filtering traditionally associated with HVDC converters stations, as well as reduces the cost and footprint of such stations considerably. This allows for application of HVDC stations in space constrained locations, e.g. in urban areas and on offshore platforms.

Lowered Switching Frequency

As the submodules in the string are series-connected, the string voltage equals the sum of the individual submodule output voltages. This means that the string can have a comparably high equivalent switching frequency while the actual switching frequency of the individual submodules can be very low. This results in a drastically reduced requirement on the switching frequency of the submodules and the semiconductor switch devices.

Optimized Valve Voltage

Already from the beginning of solid state valves there has been a balance between conduction losses and switching losses. This trade-off exists in all switch devices but is perhaps most evident in bipolar devices where the carrier lifetime has a direct impact on this trade-off. In bipolar devices the conduction and switching losses have a quite strong dependence on the allowable blocking voltage. In a cascaded converter the application voltage and the submodule, and hence device voltages, are largely decoupled and the submodule voltage rating can be chosen to optimize the overall losses.

Modular Structure and Fault Tolerance

The modular structure of most cascaded converters allows for improved reliability by addition of redundant modules. The modular structure is also beneficial from a manufacturing and testing stand-point.

The main disadvantage of cascaded converters is the need to store large amount of energy in the submodule capacitors. In M2Cs there is significant energy ripple of fundamental frequency, which is not the case in conventional two- or three-level three-phase converters where there is a cancellation of the fundamental ripple between the phases. This drawback is also shared by the CHB STATCOMs, but in that case the lowest frequency ripple is twice the line frequency. A further drawback of cascaded converters is the relatively complex control structure and the need for a large number of inputs and outputs to control the submodules. The low cost of control and computational power today limits the significance of this drawback but it can be prohibitive for power converters with low power ratings.

Although some systems can have a superficially modular structure, not all such systems exhibit all the advantages of a fully modular converter. To be fully modular the modules should have similar operating conditions, that is, the conditions for one module is not fundamentally different from the conditions of another cell. However, the modules do not need to be exactly the same, i.e. matched, but the external conditions of the modules should be equivalent.

Cascaded converters are in some sense both a natural development of earlier converter topologies and at the same time a quite different converter structure with new challenges to be solved. Among these challenges is the efficient and robust control of a large number of submodules, i.e. to control the voltage/charge balance of individual submodules as well as converter strings. This has been the topic of a large part of the research on cascaded converters and while there may remain work to be done it has been shown that there are viable solutions with adequate performance. A further issue is the requirement that submodules must go into a short-circuit in case of failures. In addition to the cascaded H-bridge and modular multilevel converters which have already been used in real-world applications [5, 8] there is a multitude of proposed converter topologies which share the same string-

of-submodules structure and the associated advantages, e.g. the modular matrix converter and the hexverter [9, 10].

In the following chapter different semiconductor devices are discussed in relation to their applicability to high-power cascaded converters.

Chapter 3

Power Semiconductors in Cascaded Converters

Silicon-based solid state power devices have been the dominating switches in almost all switch-mode valve applications for the last fifty years or so. Recently, wide band-gap (WBG) devices have started to find commercial application, but the market penetration is still small. The characteristics and performance of a switch device, whether in silicon or in a WBG semiconductor material, is greatly affected by the blocking voltage rating of the device, e.g. a bipolar device with high blocking voltage rating can achieve lower relative conduction losses but has more switching losses than a device with a lower voltage rating.

Cascaded converters bring an extra degree of freedom in the choice of semiconductor voltage rating. With other converter topologies the valve voltage is directly dependent on the application, and in higher voltage applications semiconductor devices need to be connected in series to achieve sufficient valve blocking voltage. In cascaded converters on the other hand, the valve voltage can be chosen freely without direct dependence on the application voltage. In cascaded converters there is thus a trade-off between valve blocking voltage and number of submodules. The number of submodules and the blocking voltage can be chosen to achieve optimum performance and cost. However, as there is a certain power- and voltage-independent cost associated with each submodule there is an incentive to choose high blocking voltages in order to reduce the number of submodules. This is most important in high voltage converters, e.g. HVDC converters, which have a large number of submodules even when semiconductor devices with the highest voltage ratings are used. Conversely, there is an incentive to choose lower voltages to increase the number of submodules in converters with a low number of levels in order to reduce the requirements on filtering. In an industrial application the performance will be evaluated in relation to the cost of the device. However, as it may be difficult to get good cost estimates other metrics are often used instead, e.g. the active semiconductor area. For devices based on fundamentally different technology, e.g. chip

vs. wafer devices or silicon vs WBG devices, such comparisons may be misleading as the cost structures are also fundamentally different. Another alternative is to compare devices based on the ratings given by the manufacturers. Such nominal ratings are of course somewhat arbitrary and subject to impact from marketing etc. However, due to market forces it can be assumed that devices of similar ratings and performance will have comparable prices.

There is a multitude of different device types, which differ not only in fundamental operation but also in control signal interfacing, packaging, failure modes etc. Most of these can be divided into either unipolar or bipolar devices depending on the current conduction mode, and from this simple distinction many of the characteristics can be deduced. In semiconductor switch devices the behavior in the on- and off-states are tightly coupled. In the off-state the blocking voltage capability is provided by a region devoid of free carriers, i.e. a depletion region. In all but the lowest voltage devices the depletion layer extends through a region with low doping. In the on-state the carriers drift through this low-doped region, which gives rise to the majority of the conduction losses. In unipolar devices, such as metal-oxide-semiconductor field-effect transistors (MOSFETs), the current is carried through the depletion region by majority carriers only, while in bipolar devices, e.g. insulated-gate bipolar transistors (IGBTs) and integrated gate-commutated thyristors (IGCTs), also minority carriers take part in the conduction.

3.1 Unipolar Devices

Unipolar devices depend on majority carriers, generally electrons, to carry the current in the on-state. The forward voltage drop in the on-state is linearly dependent on the current, i.e. resistive in nature. For a conventional MOSFET structure, as shown in Fig. 3.1, the resistance of the drift region is proportional to the breakdown voltage to the power of 2.4-2.6. For super-junction (charge-coupled) devices, which have a rectangular field and allow higher doping, an almost linear relation between on-state resistance and breakdown voltage can in theory be achieved [11]. In practice the on-state resistance dependence on the blocking voltage lies somewhere in between. As an illustration of this dependence Fig. 3.2 shows the typical on-state resistance vs. blocking voltage for MOSFETs in a particular package, in this case TO-263 (D2PAK). In the lower voltage range the resistances of the channel and package have a significant impact. The line shows a least-squares fit to the lowest on-state resistance in each voltage class and has a slope of approximately 2.2. Silicon MOSFETs are likely to be competitive only in the lower voltage range in applications where the granularity of devices with higher voltage ratings would be a drawback. They could maybe also find use in applications where the efficiency is at a premium or in low power applications in which bipolar devices would not be fully utilized.

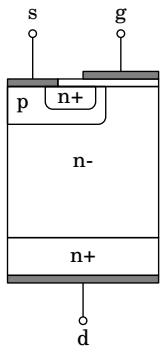

Figure 3.1: MOSFET structure cross-section.

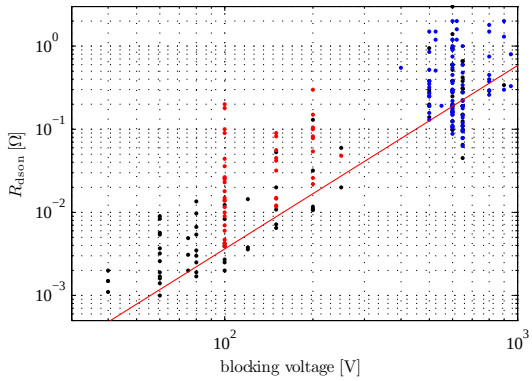

Figure 3.2: MOSFET on-state resistance vs. blocking voltage, TO-263 (D2PAK) package.

3.2 Bipolar Devices

The main drawback of unipolar devices such as the MOSFET is the high on-state voltage of devices with high blocking voltages. The voltage drop can be improved by bipolar conduction, i.e. injection of minority carriers into the depletion region.

Insulated Gate Bipolar Transistors

The Insulated Gate Bipolar Transistor (IGBT), shown in Fig. 3.3, is a direct development of the MOSFET which provides minority carrier injection and can, therefore, achieve much lower on-state voltage in high-voltage devices. In the on-state, as the forward voltage exceeds a certain threshold voltage minority carriers are injected into the depletion region, whereby the effective conductance is increased. This allows the IGBT to achieve low conduction losses also for high blocking voltages. One drawback of this *conductivity modulation* is that it increases the switching losses. This limits the application of hihg-voltage IGBTs to fairly low switching frequencies. However, in most cascaded converters this is not a significant limitation and for most applications IGBTs optimized for low conduction losses, i.e. with long carrier lifetimes, are appropriate.

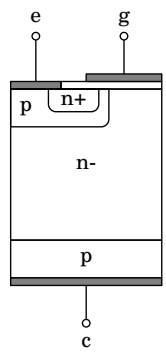

Figure 3.3: IGBT structure cross-section.

Development of the IGBT has led to devices which achieve a fairly rectangular field distribution in the off-state which allows for thin depletion layers and low conduction losses. However, a large part of the on-state voltage drop is in the region close to the emitter, i.e. close to the top side. This is due to an unfavorable carrier distribution in this region. Close to the collector the current is carried both by electrons injected through the channel and by holes from the collector. However, closer to the emitter the current is carried by either charge carrier only. Under the emitter contacts only electrons contribute to the current conduction while under the gate contacts almost only hole current flows. This lateral disposition gives rise to slightly higher conduction losses than for bipolar devices achieving balanced bipolar current flow throughout the depletion region, e.g. thyristor-type devices. This is more or less a fundamental limitation of the IGBT. However, there has been a lot of development to improve the on-state voltage, e.g. deep-trench technology and Injection-Enhanced Gate Transistors (IEGT).

Gate-Commutated Thyristors

The GCT, shown in Fig. 3.4, is a development of the gate turn-off thyristor (GTO), mainly developed to reduce the amount of passive components required [12]. As the name implies, in a GCT the full anode current is commutated to the gate during turn-off. This requires a powerful gate drive circuit capable of diverting multiple kiloamperes from the cathode to the gate within a few microseconds in order not to destroy the device. This necessitates a special gate driver with low inductance connection to the gate, which is why GCTs are generally supplied with the gate driver integrated as a so called IGCT.

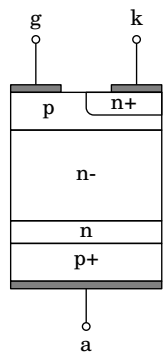

Figure 3.4: GCT structure cross-section.

Being a thyristor, the GCT has high carrier injection and good plasma distribution in the on-state and does not suffer from the lateral disposition limitations of the IGBT. It can, therefore, achieve very low on-state voltage drop. In fact, thanks to the gate drive unit, the GCT can be optimized for low conduction losses without significant penalties in turn-off capability and can, therefore, achieve lower conduction losses than GTOs and other bipolar devices such as IGBTs. A drawback of the GCT, as it is a thyristor-type device, is that the turn-on cannot be controlled to limit the rate of the current rise and also that there is no current-limiting mechanism as in IGBTs. The rate of rise in current must be limited in order to limit uneven current distribution before all thyristor cells are turned on. It must also be limited in order to allow the diode carrying the current to turn off reliably. This second consideration is generally the limiting factor.

3.3 Wide Band-Gap Devices

Wide band-gap devices utilize semiconductor materials, mainly silicon carbide (SiC) and gallium nitride (GaN), which have larger band-gap and improved characteristics compared to silicon [11]. Whereas GaN is best utilized in devices with blocking voltages below 1 kV, SiC could be used in devices potentially reaching blocking voltages in excess of 10 kV. While high voltage SiC devices have been made [13], currently available, commercial devices have blocking voltages below 2 kV. In this voltage range the relative voltage drop is arguably too high to compete with the low conduction loss of silicon devices with higher voltage ratings. However, as SiC devices are generally of the unipolar type, the conduction loss can be reduced by an increase in active area. The main advantage of WBG devices is a reduction of switching losses, allowing higher switching frequencies and a reduction of passive component sizes. In cascaded converters the passive components are largely determined by fundamental frequency relations and increased switching frequency is of little use. Therefore, in most cascaded converters the switching frequency capability of WBG devices would not be fully utilized. However, this may change as SiC technology matures and higher voltage devices become available.

3.4 Loss comparison

Depending on application, all the different semiconductor devices discussed above could find use in cascaded converters. A particular device type would likely be used in submodules with ratings similar to non-cascaded converters where such devices are applied. The main difference is the much lower switching frequency requirement due to the interleaving quality of cascaded converters. Hence, the devices used in cascaded converters will likely primarily be optimized for low conduction losses. As an illustration of the conduction losses Fig. 3.5 shows the relative forward voltage drop of a number of devices. It shows the forward voltage divided by a nominal voltage which is the typical direct voltage stress that will be applied to the device in question. The relative forward voltage is shown as a function of forward current, also normalized to nominal current. Thus this graph is directly dependent on device ratings, which is based on the assumption that the device ratings are a useful measure of device cost. Although significant uncertainty exists, and the curves in Fig. 3.5 can shift slightly, qualitative conclusions can still be drawn from it. For example, the very low conduction losses of the GCTs cannot be matched by IGBTs, even if IGBTs with much higher current ratings are used.

From the discussion above it could be assumed that the GCT would be a competitive alternative to IGBTs for use in high power cascaded converters. Although it is clear that the conduction losses would be reduced it is not immediately clear how much this would be offset by increased switching losses. To quantify this Publication I presents a loss comparison of IGBT and IGCT implementations of three different submodule topologies. The individual loss components for half-bridge,

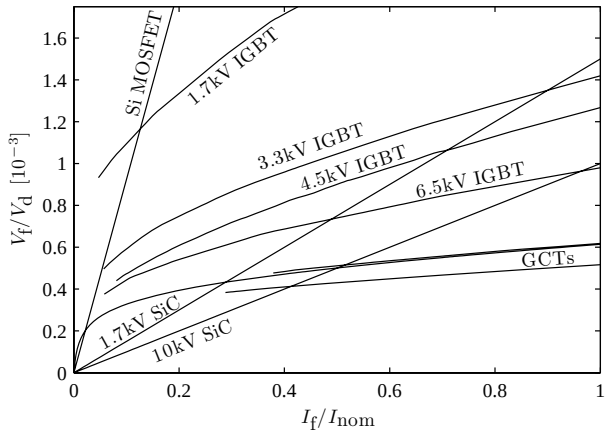

Figure 3.5: Relative forward voltage drop of various silicon devices, including IGBTs, GCTs and a 600V MOSFET as well as two SiC MOSFETs.

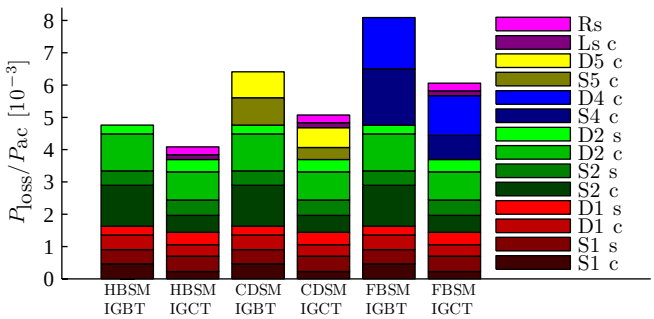

Figure 3.6: Loss comparison for IGBT and IGCT implementation of half-bridge, clamped-double and full-bridge submodules. Average of nominal power rectifier and inverter operation. Pulse number $p = 3$.

full-bridge and clamp-double submodules are shown in Fig. 3.6. The loss calculation is based on ideal voltage and current waveforms but takes into account thermal behavior, i.e. the temperature dependency, of the devices. The loss calculation method has been experimentally verified by comparing measured and calculated losses in a 10 kW demonstrator M2C as described in Publication II. The IGCT-based submodule losses include the losses in the clamp circuit, which are relatively small, but significant as they reduce the potential efficiency gain of GCT implementations. Even so, the comparison shows that GCT-based submodules could provide 20-30% lower losses than submodules based on IGBTs. To use GCTs in cascaded converters the submodules have to be designed to accommodate the special requirements related

to the GCTs. First, it must include a di/dt-reactor and clamp circuit. Second, it must include some means of supplying power to gate drive units. As GCT gate drivers require an order of magnitude more power than IGBT gate drivers this can be challenging. The supply of this power is discussed in the following chapter.

Chapter 4

Auxiliary Power Supplies

Parts of this chapter have been presented in Publications III & VI.

In cascaded converters a certain amount auxiliary power must be supplied to each submodule in order to power its control electronics and gate-drive units. Depending on the application, or rather the power and voltages involved, supplying this auxiliary power to the submodules may require some extra attention. In converters with comparably low voltages involved, up to some tens of kilovolts, as in e.g. large motor drives and transformer-coupled STATCOMs, the auxiliary power can be supplied from a ground-referenced source by means of isolation transformers [14]. In applications with higher voltages, i.e. with system voltages of hundreds of kilovolts or more, the extreme demands on isolation systems and distances makes supplying power from ground-referenced sources infeasible. Instead, the auxiliary power for the submodules must be taken from the main circuit. This can be done in some different ways, e.g. snubber energy recovery or a low-frequency transformer in series with the submodule. Arguably, the most attractive solution is to supply the auxiliary power from the submodule energy storage capacitors, as this power source is available regardless of converter operation and capacitors stay charged also during blocking of the converter. The main challenge of this solution is that it requires a dc-dc converter capable of an input voltage in the multiple-kilovolt range.

In submodules with comparably low capacitor voltages or with low power requirement (i.e. IGBT-based) a linear power supply is a simple and reliable solution as long as the low efficiency and associated power loss is acceptable. By using a shunt-type linear regulator, as opposed to series, the input voltage can be reduced by reliable resistor elements and the use of semiconductors with high blocking voltages can be avoided. In high-voltage, or high-power applications the low efficiency may be unacceptable, and to get higher efficiency some form of switching converter is needed.

4.1 Switch-mode Converters

Arguably, the simplest switching converter alternative would be a buck-type step-down converter. With the demand for very large conversion ratios, converters which also provide a turns-ratio voltage conversion, e.g. tapped inductor-buck or flyback converters, may be better alternatives. Such converters can provide a higher duty ratio and hence better switch utilization and efficiency. However, the most important issue is how to accommodate the high input voltage, as for most topologies this requires one or more valves capable of blocking voltages equal to or exceeding the input voltage. While semiconductor devices with adequate blocking voltages exist, e.g. devices used in the submodule main valves, these may not be suitable in the auxiliary power application as voltage and power levels generally go hand in hand. The input voltage in the multiple-kilovolt range would imply power levels in the tens if not hundreds of kilowatt range. This means that most semiconductor switch devices which fulfill the required blocking voltage have current ratings exceeding the auxiliary power supply requirement by orders of magnitude. By series connection devices with lower voltage ratings can be used, but this introduces new issues related to the series connection. The two most important problems to be solved are the supply of gate signals and power to the individual devices and ensuring adequate sharing of the blocking voltage among the devices. Pulse transformers are the most readily available option to provide gate-drive isolation in high voltage applications. However, in a converter with a series-connected valve a comparably large number of galvanic isolation barriers are needed and due to the cost and size of pulse transformers this is a significant drawback in high-voltage, low-power dc-dc converters. In Publication III a tapped-inductor buck converter is introduced which uses a novel high-voltage valve in which the voltage sharing and gate drive control is realized without the use of pulse transformers or isolators.

4.2 Tapped-inductor Buck Converter

The tapped-inductor buck converter [15, 16], shown in Fig. 4.1, has numerous advantages in high-voltage applications, especially in converters with series-connected valves. First, due to the inductor turns-ratio it can achieve a comparably high duty ratio and efficiency. Second, it can provide quasi-resonant commutations with zero voltage switching (ZVS) by means of current-injection [16]. This is beneficial in high voltage converters where the parasitic capacitance of the valves can otherwise give rise to large switching losses, and it allows for large snubber capacitors in the valve to improve voltage sharing among the switch devices without large penalties in terms of losses. Also, in the converter described in Publication III a novel high-voltage valve is used which depends on this ZVS operation of the converter. The turn-on of the devices in the valve is initiated by the zero-voltage condition, or rather by the reverse bias of the valve. Each switch device is turned on individually as this condition is sensed and the reverse bias is also utilized to provide local gate-drive power. To

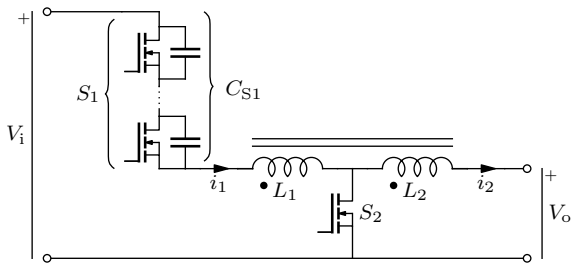

Figure 4.1: Tapped-inductor buck converter with a high-side valve, S_1, consisting of several series-connected MOSFETs.

avoid the use of galvanic isolation components also the turn-off is initiated by the valve in peak-current control fashion. This peak-current control precludes the use of conventional pulse width modulation and instead a variable switching frequency is used to control the power transfer. The control method and structure is described in Publication V which also describes the start-up behavior of the converter. A photograph of the 3 kV, 70 W tapped-inductor buck converter is shown in Fig. 4.2. Note that there are no additional connections to the high-voltage valve except for the positive and negative power terminals. In a tapped-inductor buck converter, as

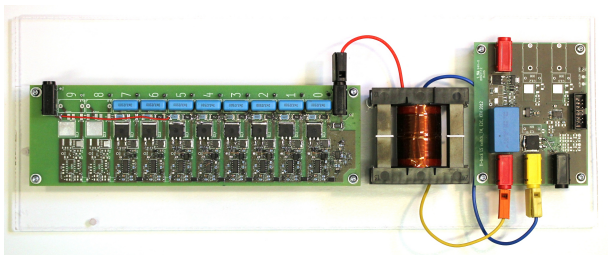

Figure 4.2: Photograph of a 3 kV, 70 W tapped-inductor buck converter. High-side valve on the left, tapped-inductor in the middle and low-side valve on the right.

in flyback converters, the leakage inductance of the inductor has a negative impact on the converter performance. If it is too large, capacitive snubbers may have to be added in order to avoid over-voltages, which reduces the efficiency of the converter. Therefore, an inductor is needed which provides both sufficient isolation and low leakage. Publication IV describes a tapped inductor wound on a standard core and coil former which has adequate isolation and leakage inductance below 1%, which means that no snubber is needed across the low-side valve. With this inductor and an input voltage of 3 kV the converter achieves efficiency of over 80% and adequate voltage sharing among the devices in the high-voltage valve. Figure 4.3 shows a

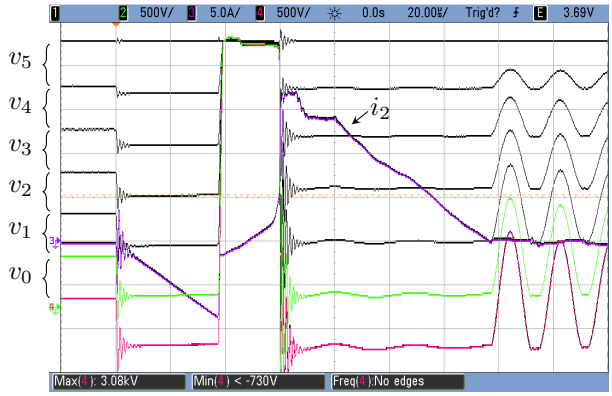

Figure 4.3: Voltage and current waveforms for TI-buck converter with 3.0 kV input voltage. The voltages over the individual switch cells can be seen as the differences between the traces, indicated as v_0 through v_5.

commutation cycle of the converter where the voltage over each device can be seen. Due to the peak-current control of the converter, for a certain input voltage each switching cycle is essentially the same regardless of the power. In Fig. 4.3 the voltage sharing among the devices is adequate, but this depends on strict timing of the turn-off of the individual devices. In valves with a larger number of devices ensuring this timing and voltage sharing can be difficult, whereby the number of devices in the valve, and hence also the input voltage of such a solution is limited. It can be alleviated by lowering the voltage derivative during commutation, but this leads to lower switching frequencies and an increase in cost of passive devices, i.e. inductor and snubbers. Another option is to connect converter stages in series instead of individual switch devices, whereby the strict timing requirements are mitigated. Two such converters proposed for the high voltage step-down applications are the series-input parallel-output converter and the so called rainstick converter.

4.3 Series-input Parallel-output Converters

By connecting the inputs of several isolated DC-DC converters in series, as shown in Fig. 4.4, the high input voltage can be handled by relatively conventional converters [17, 18]. While some precautions must be taken to ensure voltage balancing among the converters, this is considerably simpler than the balancing of individual switches as the timing requirements are lower. With converters without active voltage control on the input side the power of the converters must be controlled so that the input voltage is evenly shared among the converters. This can be done in an active fashion, or it can depend on passive mechanisms such as converter losses and resistive voltage dividers. In [17] commercial converters with a current mode

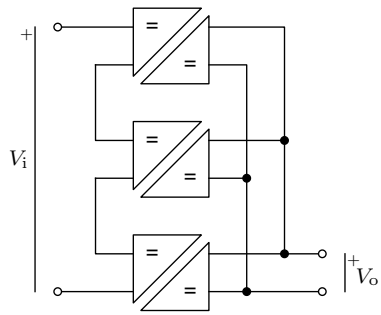

Figure 4.4: Series-input parallel-output isolated dc-dc converters

for parallel connection are used to operate the converters in an equal power mode and use an active balancing circuit with opto-couplers to control the converters. In [18] flyback converters are used with synchronized and equal gate signals, also using opto-couplers, such that the input voltage directly affects the power transfer. Another option would be to use converters which directly reflect the output voltage in the input, i.e. in a dc transformer fashion. A drawback of the series-input parallel output solution is that a number of transformers with high voltage isolation are needed, as opposed to just one in the tapped-inductor buck converter.

4.4 Rainstick Converter

The zig-zag, or rainstick [19], converter shown in Fig. 4.5 removes the need for high voltage isolation transformers by cascading non-isolated converter stages. Superficially, the rain-stick converter looks somewhat similar to the series connection

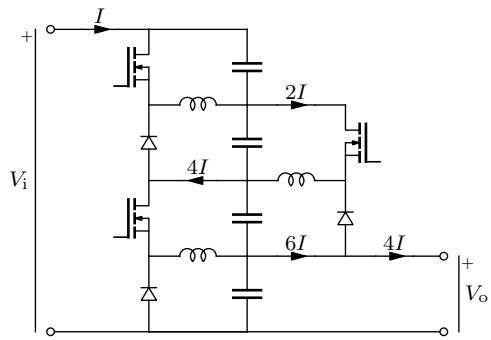

Figure 4.5: "Rainstick" converter.

in a cascaded converter. However, as the output of one stage is the input of the next, the stages are in a true cascaded structure, i.e. the output of one stage is the input of the next, rather than just connected in series as in CHBs or M2Cs. This implies that the overall efficiency is the product of all the individual stage efficiencies, which puts quite strict requirements on the efficiency of the individual stages. As the converter stages operate at a fixed conversion ratio of 0.5, i.e. the limit for ZVS without current injection, it should be possible to achieve comparably high efficiency for the individual stages also at high switching frequencies despite the high voltages involved. A result of the cascaded structure is that the current magnitude is not the same for all stages, but rather increases linearly along the cascade, i.e. the conditions for a stage near the top of the cascade is quite different from those of a stage further downstream. Therefore, the design of the stages does not lend itself very well to a modular structure.

Chapter 5

Submodule Test Circuit

Parts of this chapter have been presented in Publications VII & VIII.

Cascaded converters have gathered a lot of interest for use in very high-power converters. Arguably, it can be expected that not only will this interest continue but also that cascaded converters will be considered in other applications, and power ranges, where the benefits are similar. Therefore, further development of cascaded converters will continue in the coming years, if not decades. Cascaded converters owe much of their advantages to the modular structure. The modular structure also suggests that testing of the converter can be performed on a single, or a small number of submodules, while providing results valid for the whole converter. This is an advantage compared to other, non-modular, converters where typically a whole converter or phase-leg must be built in order to allow testing. While a lot of information can be gained from pulse tests, e.g. regarding the commutation behavior, other issues may require test circuits allowing continuous operation. Most importantly losses and efficiency are best evaluated under conditions as similar to the real application as possible. In this chapter a few alternative test circuits for continuous operation are discussed.

5.1 Test Circuit Topologies

In a cascaded converter the switching of an individual submodule has very little impact on the current through it, i.e. from the perspective of a submodule the converter behaves as a current source. Therefore, in theory the simplest test setup would be a current source connected to a single submodule as shown in Fig. 5.1. While such solutions have clear advantages and have been proposed [20], providing such a current source for high-power submodules may prove difficult due to the pulsed operation and large voltage derivatives.

An alternative test circuit which does not require a high-performance current source amplifier is a series-resonant test circuit such as shown in Fig. 5.2. In such a

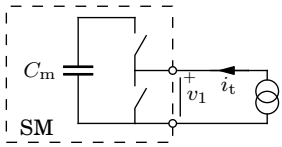

Figure 5.1: Submodule connected to a current source for testing.

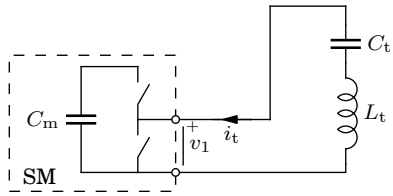

Figure 5.2: Single submodule series-resonant test circuit.

circuit the current can be controlled by the submodule under test and the resonant circuit provides low impedance at the fundamental while attenuating the switching ripple current. While conceptually simple, this type of test circuit has some significant drawbacks: First, power to match the losses must be fed into the submodule which requires extra connections, e.g. to the dc-link capacitor. Second, the current in the test circuit and the submodule output voltage are directly coupled. Third, the inductance must be large in order to limit current ripple and also to limit the impact of the submodule switching on the resonance frequency. These drawbacks can be mitigated by the addition of a second submodule and an external power source as shown in Fig. 5.3. This type of circuit, which is described in Publication VII, derives

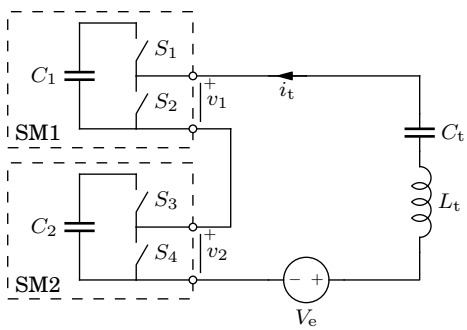

Figure 5.3: Series-resonant test circuit with two submodules to achieve cancellation.

many advantages by switching the submodules in opposition, or near opposition. The advantages are: First, the voltages from the submodule cancel to a large degree, which reduces current ripple. Second, the impedance of the circuit stays essentially the same with respect to the switch state. Third, the test current and submodule output voltage are decoupled, allowing current and voltage dependencies to be investigated separately. Fourth, the reactive powers of the submodules can be made to cancel out so that the power source only supplies the power losses. Fifth, most

failure modes offset the resonance and the resulting currents and voltages are limited in amplitude. Related to the last items is also the possibility to test high power submodules using a low-power source, which is beneficial in terms of cost but also as it limits the short-circuit power in case of failures.

5.2 Control Structure

The control structure, shown in Fig. 5.4, used to run the test circuit and achieve the stated benefits is described in the following. The modulation of the submodules

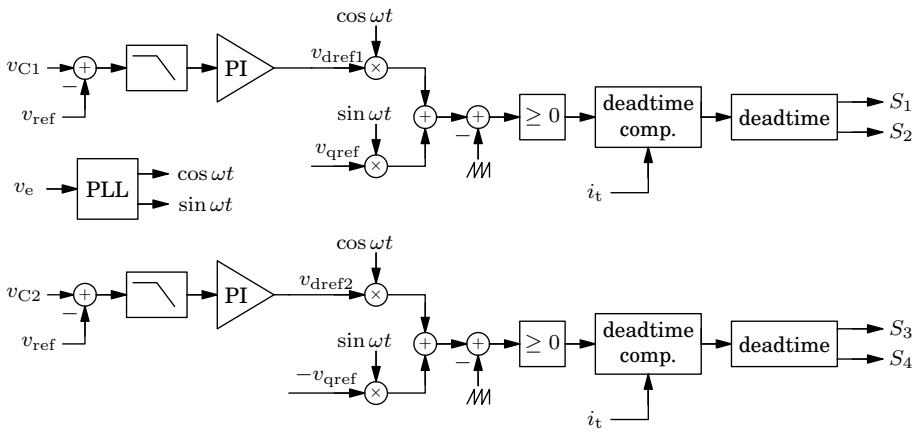

Figure 5.4: Resonant test-circuit control structure.

is synchronized to the excitation voltage by means of a phase-locked loop (PLL). The PLL uses a variable timer increment to provide a fundamental phase angle counter of length 2^n, which simplifies the generation of in-phase sine and cosine signals. These signals are used in the pulse width modulation loop (PWM) block to provide direct control of in-phase (d-) and quadrature (q-) voltage components. The PWM block uses the same phase increment as the PLL, scaled by the pulse number. This guarantees synchronism between the two counters, while allowing on-the-fly changes to the pulse number without spurious pulses. The reactive component of the submodule voltages can be set via a user interface. The submodules provide reactive powers of opposite signs, as illustrated by the phasor diagram in Fig. 5.5, such that they cancel to a large degree. This limits the reactive power needed from the test circuit excitation source. Small active power components in the submodule output voltages are introduced to allow balancing and control of the submodule capacitor voltages. The pulse generation and protection is synthesized in logic of a field-programmable gate array (FPGA) while the control, i.e. capacitor voltage

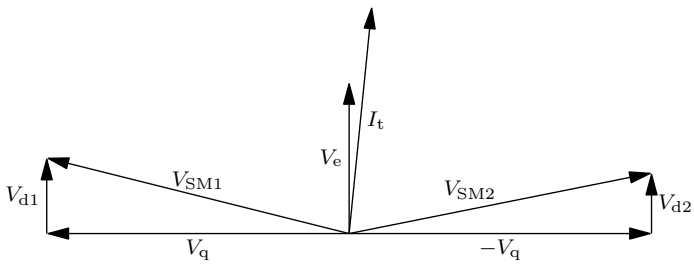

Figure 5.5: Phasor diagram of test circuit quantities.

controllers and PLL loop filter, is run on a softcore-processor implemented on the same device.

While some dead-time between the turn-off of one valve and the turn-on of the other is absolutely necessary, this has some negative impact on the test circuit operation. During the dead-time the submodule output voltage is determined by the current sign. As this voltage is always opposing the current this provides quite effective damping. To reduce this unwanted impact a dead-time compensation block is introduced which controls the instant of the voltage transition by delaying the turn-off and turn-on signals depending on the current sign. The dead-time compensation introduces a small phase shift which results in some cross-coupling between the d- and q-axis. In practice this has negligible effect as the d-axis reference is small and, therefore, has little impact on the q-component, and the q-axis coupling to the d-axis is compensated by the capacitor voltage controllers.

5.3 Calorimetric Loss Measurement

All the components in the submodules which have significant power losses are cooled by a closed-loop de-ionized water system. This allows for calorimetric measurement of the power losses by measuring water flow and inlet and outlet temperatures. As the submodules are not specifically designed for calorimetric measurements there is significant thermal coupling between the devices and measuring the losses in an individual device is difficult. However, measuring the total losses in the submodules is comparably simple and straightforward. The flow is measured by a variable area meter and assumed constant throughout the measurements. The inlet and outlet temperatures are measured by K-type thermocouples. The small size allows the thermocouples to be inserted into the water without impeding the flow.

The calorimetric setup was calibrated in three steps: First, the offsets in the temperature measurements were nulled by connecting the thermocouples to a isothermal copper block. Second, an equivalent thermal resistance between the water cooling system and the ambient air was measured by running warm water

through the cooling system and measuring the temperature difference between inlet and outlet. This thermal resistance could then be used for a first-order compensation of the heat loss to the ambient. Third, a known loss was dissipated in the diodes of one submodule by passing a controlled direct current through them. As the thermal resistance between the different parts of the system is low, this concentration of losses to just three devices does not affect the loss measurement considerably. The response of estimated power in the calorimetric setup during a test sequence is shown in Fig. 5.6. It shows the estimated loss calculated using the inlet and outlet

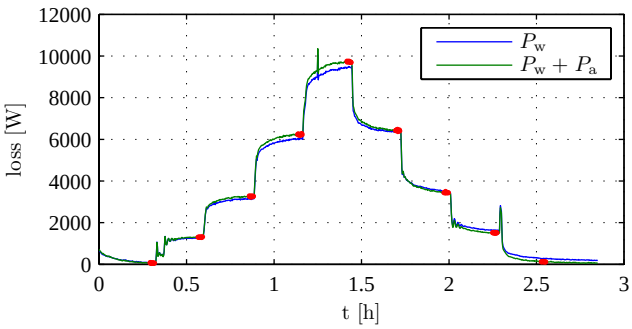

Figure 5.6: Calorimetric measurement power loss.

temperatures without and with compensation for the heat flow to the ambient air. The samples highlighted in red are used in the loss comparison presented in the following chapter.

Chapter 6

Experimental Results

Parts of this chapter have been presented in Publications VII & VIII.

From the loss comparison in Publication II it can be expected that the use of GCTs in cascaded topologies should allow for converters with very low losses. In order to verify that this is really the case, two GCT-based submodules were designed and built for testing. By building full-scale submodules it is also shown that it is viable to build high-power submodules, and hence cascaded converters, using GCTs. The submodule design, which is described in Publication VIII, is based on asymmetric GCTs with blocking voltage rating of 4.5 kV. A circuit diagram of the submodule structure is shown in Fig. 6.1, which in addition to the GCTs (T_1, T_2) shows the anti-parallel diodes (D_1, D_2), the dc-link capacitor (C_m), the di/dt-reactor (L_cl) and associated clamp circuit (D_cl, R_cl, C_cl). A photograph of

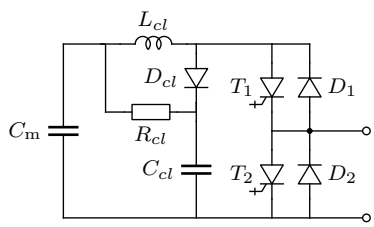

Figure 6.1: IGCT-based half-bridge submodule.

one of the submodules is shown in Fig. 6.2 with designations corresponding to the circuit diagram in Fig. 6.1. Two such submodules were built in order to allow testing in a two-submodule resonant circuit as described in the previous chapter. One of the prominent advantages of the test circuit is the low harmonic content of the current also for low pulse numbers. This is evident in Fig. 6.3 which shows waveforms from the test circuit when running at 1.4 kA and with a pulse number $p = 3.125$. Even

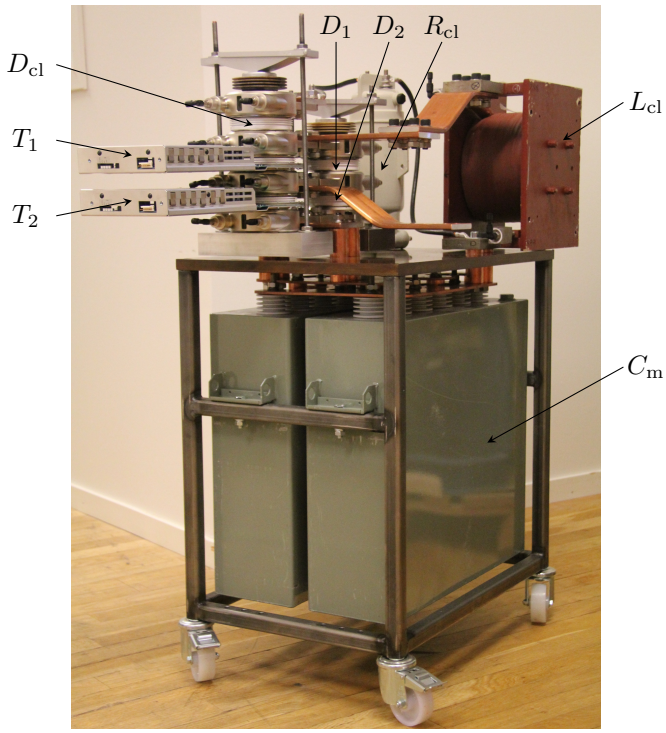

Figure 6.2: IGCT-based cascaded converter cell showing the main components with designations in reference to Fig. 6.1. The clamp capacitor, C_{cl}, is located behind the stacks and not visible.

though the capacitor voltage ripple is almost 1 kV, the test-circuit current has a total harmonic distortion (THD) of less than 10%. Also evident is the high power factor at the terminals of the excitation source. When correctly tuned the source only has to supply little reactive power and also very little harmonics. The gate signals for the two submodules are visible at the bottom of the figure. Due to the fractional pulse number the gate pulses shift slightly between each fundamental cycle and repeat after eight cycles. This is hardly visible in the gate pulses shown in Fig. 6.3 but can be perceived in the capacitor voltage waveforms.

A more detailed view of the commutations within a submodule is shown in Fig. 6.4 and Fig. 6.5. Figure 6.4 shows the anode current and voltage across the low-side GCT as it turns on. As the GCT turns on, the voltage across it, v_{ak}, falls to zero within less than 1 μs after which the current rise is governed by the di/dt-reactor. Also visible is considerable diode reverse recovery. Fig. 6.5 shows the turn-off, and although the submodule capacitor voltage is only 1.8 kV at turn-off the voltage across the GCT reaches 2.8 kV during the clamping process. This is

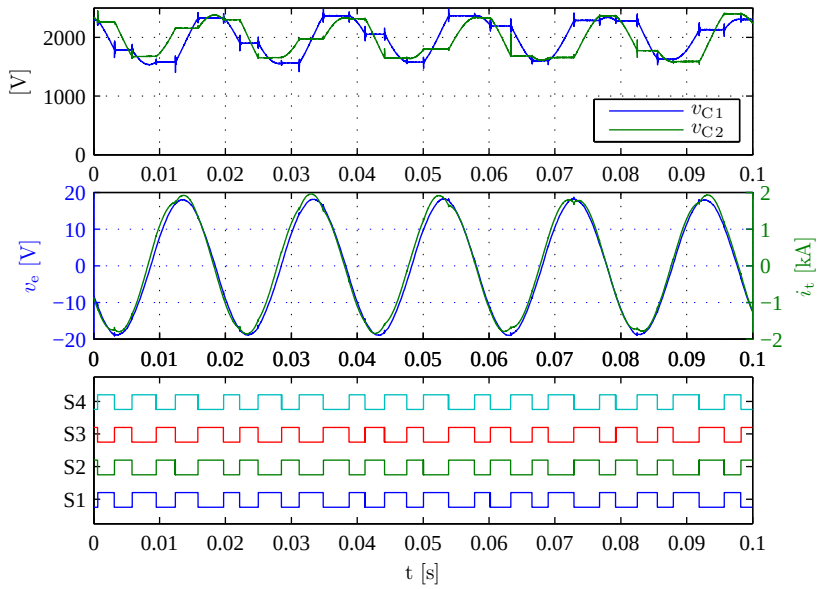

Figure 6.3: Waveforms from the test circuit in steady-state operation. The average capacitor voltage is 2 kV, the test current is 1.3 kA, and the pulse number is 3.125.

close to the acceptable limit for this type of GCT in order not to reduce the lifetime due to cosmic radiation. Therefore, it limits the average capacitor voltage to 2.0 kV to allow turn-off commutations at 2.0 kA. The peak voltage could be reduced by an increased clamp capacitance, or by reducing the clamp inductance as the di/dt during turn-on (380 A/μs) is well below the ratings of both GCTs and diodes.

To compare the losses from the calorimetric measurements with the simulations the test setup was run at a few different current levels and two different pulse numbers. The current is set manually by adjusting the excitation voltage and is, therefore, difficult to adjust to an exact value. The pulse number on the other hand is exact, but changes to it affects the current as the losses in the circuit change. Therefore, it was decided to use test sequences in which the pulse number is kept constant and adjust the excitation to a number of approximate current magnitudes, rather than varying the pulse number and trying to adjust the current to an exact value. In Fig. 6.6 calorimetric measurement results from two such test sequences for pulse number 3.125 and 5.125 are shown. Also shown in the figure are the losses calculated using the method presented in Publication I. Although there is a significant discrepancy, around 7% or 0.7 kW at 1.2 kA, it still shows acceptable correspondence between simulations and measurements. The exact nature of this discrepancy has not been determined, but one likely cause is that the measurements include losses that are not included in the simulation. It should be noted that

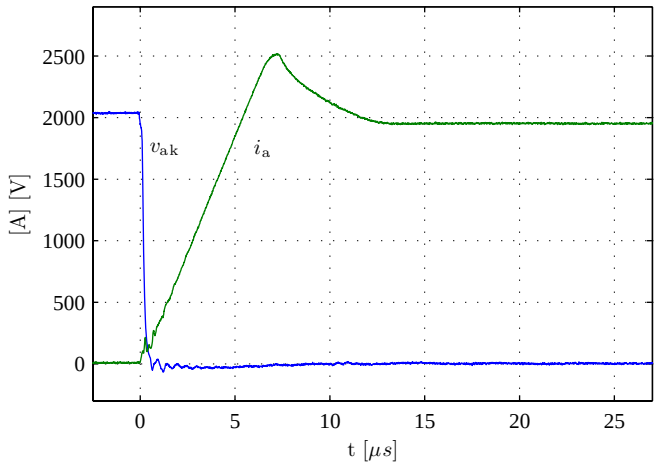

Figure 6.4: Turn-on of the low-side GCT showing anode-cathode voltage, v_{ak}, and anode current, i_a.

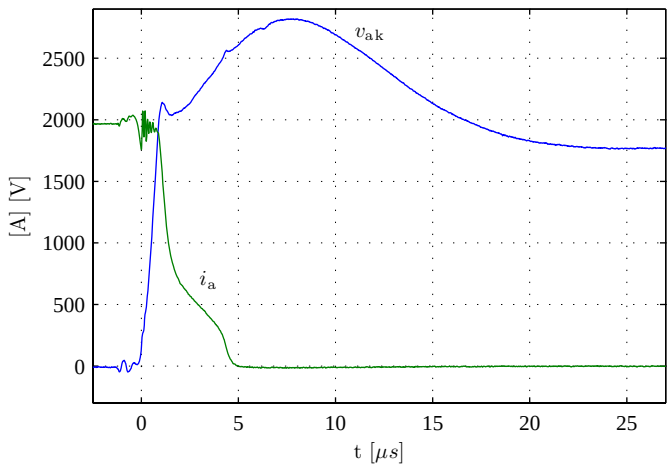

Figure 6.5: Turn-off of the low-side GCT.

at 1.2 kA the submodule losses only constitute about half of the total losses in the test circuit, while the rest is mainly losses in the cabling and the test-circuit reactor. If any of these other losses are transferred to the cooling water, it could explain the somewhat higher measured losses than expected from the simulations. The measurement and simulation is in quite good agreement at low current, and the difference has a largely quadratic, or resistive, dependence on the test current

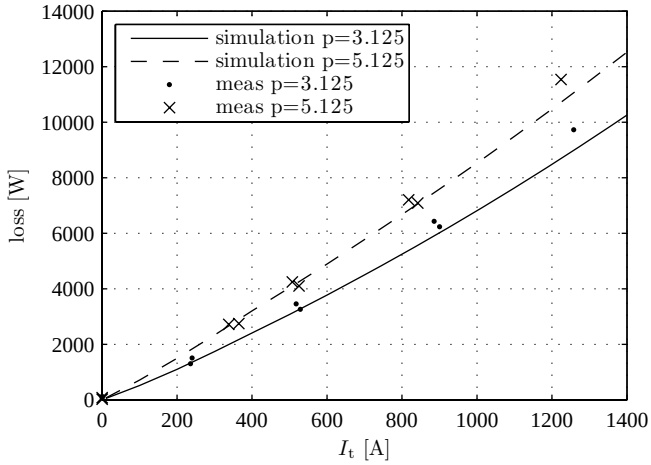

Figure 6.6: Comparison of calculated losses and losses estimated from the calorimetric measurement.

with a corresponding equivalent resistance of only 0.5 mΩ. The conditions in the test circuit are not exactly the same as in a real application, most notably the dc bias and the active power component are missing in the current. While this is a drawback, this type of circuit benefits from the fact that essentially all submodule losses are included as is. Therefore, there is no need to extrapolate or assume certain loss components. Furthermore, the results show that there are no large unknown loss components or mechanisms that impact efficiency appreciably.

With this vindication of the loss comparison from Publication II it seems very likely that in the near future high-power cascaded converters will use GCTs as the efficiency gain (20-30%) compared to IGBTs is too large to ignore.

Chapter 7

Conclusions

This thesis started as an investigation into the use of GCTs in cascaded converters, as it could potentially lower the losses. The low conduction loss of GCTs is seldom disputed, but it is sometimes argued that the potential efficiency gains are offset by losses in the diodes or clamp circuit. The loss calculations and the results from tests performed on full-scale submodules show that this is not the case at low switching frequencies. Therefore, GCTs can achieve superior efficiency at low switching frequencies, i.e. for pulse numbers around three. One can assume that even lower switching frequencies will be used in large cascaded converters to minimize losses [21], which accentuates the GCT advantages even more. Another important advantage of using GCTs is the high reliability and robustness. This is in part due to the presspack package which does not suffer from lifetime-limiting issues due to degradation of bond-wires or solder interfaces. GCTs also have excellent surge handling capability and there is little risk of explosive failures.

The resonant test circuit developed to verify the loss calculations and the submodule operation has proved to be a simple and effective means of testing high power submodules. While imposing certain limitations, i.e. the lack of dc bias and active power in the submodule current, it provides acceptable conditions for steady-state testing and efficiency evaluation. Also, by identifying the few shortcomings and limitations of the test circuit it enables and simplifies the use of it in cases where the limitations are acceptable.

The supply of power for gate drive units in GCT submodules remain a challenge, especially if devices with higher blocking voltages are to be used. There is, however, a number of viable solutions, including the tapped-inductor buck converter, with autonomous high-side switch, presented in this thesis. It provides acceptable efficiency and does not depend on galvanic isolation components for the operation of the high-side valve. This type of converter could also benefit from new types of devices, i.e. SiC MOSFETs, whereby the higher input voltages and switching frequencies could be accommodated.

7.1 Future Work

The work presented in this thesis has shown that GCTs can lower the losses in high-power cascaded converters. However, much work remains in order to employ GCTs in cascaded converters for commercial applications. Much of the remaining work is of an applied development nature best performed by industry, but there are also issues that can be of academic interest, such as topological changes to the submodules. One such issue is investigating the possibility of soft-switching submodules. In addition to reducing the switching losses, soft-switching also has positive secondary effects, such as allowing diodes and valves optimized for very low conduction losses. Furthermore, while eliminating the need for the di/dt-reactor is beneficial in itself, it also allows for higher dc-link voltages as the transient voltage spikes at turn-off are avoided.

Also looking into alternative valve realizations could be interesting, e.g. the application of GCTs with integrated diodes which can simplify the main circuit of the submodules considerably. This is also the case with bi-mode GCTs [22], which, by utilizing the whole active area both in forward and reverse conduction, have the potential to improve both performance and ratings. On this topic, the application of GCTs with higher blocking voltage rating, e.g. 10 kV, could further reduce losses and cost. In this voltage range the advantages of WBG devices are more pronounced, so investigating the use of e.g. SiC devices could also be very interesting. In contrast to this, it could also be worthwhile to investigate the use of cascaded converters in applications with lower system voltages than in the existing grid applications, e.g. in voltage ranges where unipolar devices are competitive. However, this will require developing cost- and power-efficient means of control of the submodules.

List of Acronyms

CHB cascaded H-bridge converter

CSC current-source converter

FPGA field-programmable gate array

GaN gallium nitride

GCT gate-commutated thyristor

GTO gate turn-off thyristor

HVDC high-voltage direct current

MTDC multi-terminal high-voltage direct current

HEV/EV (hybrid) electric vehicle

IGBT insulated-gate bipolar transistor

IGCT integrated gate-commutated thyristor

M2C modular multilevel converter

MOSFET metal-oxide-semiconductor field-effect transistor

STATCOM static compensator

SiC silicon carbide

PLL phase-locked loop

PWM pulse width modulation loop

VSC voltage-source converter

WBG wide band-gap

ZVS zero voltage switching

THD total harmonic distortion

List of Figures

2.1 A string of submodules, the central concept of cascaded converters, showing simplified voltage waveforms of submodules and the string. Also shown is the simplified structure of a half-bridge submodule and alternative valve realizations. 7
2.2 Cascaded H-bridge static synchronous compensator (STATCOM). Also shown is the simplified structure of a full-bridge submodule. 8
2.3 Modular multilevel converter (M2C). Also shown is a half-bridge submodule, but many other submodule topologies have been proposed. . . 9
2.4 Back-to-back M2C. 10

3.1 MOSFET structure cross-section. 15
3.2 MOSFET on-state resistance vs. blocking voltage, TO-263 (D2PAK) package. 15
3.3 IGBT structure cross-section. 15
3.4 GCT structure cross-section. 16
3.5 Relative forward voltage drop of various silicon devices, including IGBTs, GCTs and a 600V MOSFET as well as two SiC MOSFETs. 18
3.6 Loss comparison for IGBT and IGCT implementation of half-bridge, clamped-double and full-bridge submodules. Average of nominal power rectifier and inverter operation. Pulse number $p = 3$. 18

4.1 Tapped-inductor buck converter with a high-side valve, S_1, consisting of several series-connected MOSFETs. 23
4.2 Photograph of a 3 kV, 70 W tapped-inductor buck converter. High-side valve on the left, tapped-inductor in the middle and low-side valve on the right. 23
4.3 Voltage and current waveforms for TI-buck converter with 3.0 kV input voltage. The voltages over the individual switch cells can be seen as the differences between the traces, indicated as v_0 through v_5. 24
4.4 Series-input parallel-output isolated dc-dc converters 25
4.5 "Rainstick" converter. 25

5.1 Submodule connected to a current source for testing. 28

5.2 Single submodule series-resonant test circuit. 28
5.3 Series-resonant test circuit with two submodules to achieve cancellation. 28
5.4 Resonant test-circuit control structure. 29
5.5 Phasor diagram of test circuit quantities. 30
5.6 Calorimetric measurement power loss. 31

6.1 IGCT-based half-bridge submodule. 33
6.2 IGCT-based cascaded converter cell showing the main components with designations in reference to Fig. 6.1. The clamp capacitor, C_{cl}, is located behind the stacks and not visible. 34
6.3 Waveforms from the test circuit in steady-state operation. The average capacitor voltage is 2 kV, the test current is 1.3 kA, and the pulse number is 3.125. 35
6.4 Turn-on of the low-side GCT showing anode-cathode voltage, v_{ak}, and anode current, i_{a}. 36
6.5 Turn-off of the low-side GCT. 36
6.6 Comparison of calculated losses and losses estimated from the calorimetric measurement. 37

Bibliography

[1] U. Raudsaar, I. Drovtar, and A. Rosin, "Overview - pumped-hydro energy storage for balancing wind energy forecast errors," in *Proc. Electric Power Quality and Supply Reliability Conf.*, pp. 133–138, June 2014.

[2] B. Zakeri and S. Syri, "Economy of electricity storage in the nordic electricity market: The case for Finland," in *Proc. IEEE Int. Conf. European Energy Market*, pp. 1–6, May 2014.

[3] C. Brancucci Martinez-Anido and L. de Vries, "Are cross-border electricity transmission and pumped hydro storage complementary technologies?," in *Proc. IEEE Int. Conf. European Energy Market*, pp. 1–7, May 2013.

[4] M. Whittingham, "History, evolution, and future status of energy storage," *Proceedings of the IEEE*, vol. 100, pp. 1518–1534, May 2012.

[5] J. D. Ainsworth, M. Davies, P. J. Fitz, K. E. Owen, and D. R. Trainer, "Static VAr compensator (statcom) based on single-phase chain circuit converters," *IEE Proceedings-Generation, Transmission and Distribution*, vol. 145, no. 4, pp. 381–386, 1998.

[6] D. Hanson, M. Woodhouse, C. Horwill, D. Monkhouse, and M. Osborne, "STATCOM: a new era of reactive compensation," *Power Engineering Journal*, vol. 16, pp. 151–160, June 2002.

[7] R. Marquardt, A. Lesnicar, and J. Hildinger, "Modulares Stromrichterkonzept für Netzkupplungsanwendung bei hohen Spannungen," in *Proc. ETG-Fachtagung, Bad Nauheim, Germany*, 2002. (in German).

[8] S. P. Teeuwsen, "Modeling the trans bay cable project as voltage-sourced converter with modular multilevel converter design," in *Proc. IEEE Power and Energy Society General Meeting*, pp. 1–8, 2011.

[9] Y. Wan, S. Liu, and J. Jiang, "Generalised analytical methods and current-energy control design for modular multilevel cascade converter," *Power Electronics, IET*, vol. 6, pp. 495–504, March 2013.

[10] K. Ilves, L. Bessegato, and S. Norrga, "Comparison of cascaded multilevel converter topologies for AC/AC conversion," in *Proc. Int. Power Electron. Conf. (IPEC)*, pp. 1087–1094, May 2014.

[11] J. Lutz, H. Schlangenotto, U. Scheuermann, and R. De Doncker, *Semiconductor Power Devices*. Springer Verlag, 2011.

[12] H. Gruening and A. Zuckerberger, "Hard drive of high power GTOs: better switching capability obtained through improved gate-units," in *Conf. Rec. IEEE Industry Applications Conf. (IAS)*, vol. 3, pp. 1474–1480 vol.3, Oct 1996.

[13] M. Das, C. Capell, D. Grider, R. Raju, M. Schutten, J. Nasadoski, S. Leslie, J. Ostop, and A. Hefner, "10 kV, 120 A SiC half H-bridge power MOSFET modules suitable for high frequency, medium voltage applications," in *Proc. IEEE Energy Conversion Cong. and Expo. (ECCE)*, pp. 2689–2692, Sept 2011.

[14] C. Marxgut, J. Biela, J. W. Kolar, R. Steiner, and P. K. Steimer, "DC-DC converter for gate power supplies with an optimal air transformer," in *Proc. IEEE Applied Power Electronics Conf. Expo.*, pp. 1865–1870, 2010.

[15] M. Rico, J. Uceda, J. Sebastian, and F. Aldana, "Static and dynamic modeling of tapped-inductor DC-to-DC converters," in *Proc. IEEE Power Electronics Specialists Conf.*, vol. 87, pp. 281–288, 1987.

[16] J.-H. Park and B.-H. Cho, "Nonisolation soft-switching buck converter with tapped-inductor for wide-input extreme step-down applications," *IEEE Trans. Circuits Syst. I, Reg. Papers*, vol. 54, pp. 1809–1818, Aug. 2007.

[17] K. Siri, M. Willhoff, K. A. Conner, and D. Q. Tran, "High-voltage-input, low-voltage-output, series-connected converters with uniform voltage distribution," in *Proc. IEEE Aerospace Conf.*, 2009.

[18] S. Senturk, T. Maerki, P. Steimer, and S. McLaughlin, "High voltage cell power supply for modular multilevel converters," in *Proc. IEEE Energy Conversion Congr. and Expo.*, pp. 4416–4420, 2014.

[19] M. Kasper, D. Bortis, and J. Kolar, "Novel high voltage conversion ratio rainstick dc/dc converters," in *Proc. IEEE Energy Conversion Congr. Expo.*, pp. 789–796, 2013.

[20] Y. Tang, L. Ran, O. Alatise, and P. Mawby, "A model assisted testing scheme for modular multilevel converter," *IEEE Transactions on Power Electronics*, vol. PP, no. 99, pp. 1–1, 2015.

[21] A. Hassanpoor, L. Angquist, S. Norrga, K. Ilves, and H.-P. Nee, "Tolerance band modulation methods for modular multilevel converters," vol. 30, pp. 311–326, Jan 2015.

[22] U. Vemulapati, M. Bellini, M. Arnold, M. Rahimo, and T. Stiasny, "The concept of bi-mode gate commutated thyristor-a new type of reverse conducting IGCT," in *Proc. Int. Symp. Power Semiconductor Devices and ICs*, pp. 29–32, 2012.

Publication I

Loss Comparison of Different Sub-Module Implementations for Modular Multilevel Converters in HVDC Applications

T. Modeer, H.-P. Nee, and S. Norrga

Published in *Proc. 15th European Conf. Power Electronics and Applications (EPE)*, 2011, pp. 1-7.

©2011 EPE Association. Reprinted with permission.

Publication II

Loss Comparison of Different Sub-Module Implementations for Modular Multilevel Converters in HVDC Applications

T. Modeer, H.-P. Nee, and S. Norrga

Published in *EPE Journal Vol. 22 no 3 September 2012*, 2012, pp. 32-38.

©2012 EPE Association. Reprinted with permission.

Publication III

High-Voltage Tapped-Inductor Buck Converter Auxiliary Power Supply for Cascaded Converter Submodules

T. Modeer, S. Norrga, and H.-P. Nee

Published in *Proc. Energy Conversion Cong. Expo.*, pp. 19–25, 2012.

©2012 IEEE. Reprinted with permission.

Publication IV

Design and Evaluation of Tapped Inductors for High-Voltage Auxiliary Power Supplies for Modular Multilevel Converters,

T. Modeer, M. Zdanowski, and H.-P. Nee

Published in *Proc. International Power Electronics and Motion Control Conference (EPE-PEMC 2012 ECCE Europe. IEEE)*, 2012.

©2012 IEEE. Reprinted with permission.

Publication V

Modeling and Control of a Tapped-Inductor Buck Converter with Pulse Frequency Modulation,

L. Bessegato, T. Modeer, and S. Norrga

Published in *Proc. Energy Conversion Congress and Exposition (ECCE)*, 2014.

©2014 IEEE. Reprinted with permission.

Publication VI

High-Voltage Tapped-Inductor Buck Converter Utilizing an Autonomous High-Side Switch

T. Modeer, S. Norrga, and H.-P. Nee

Accepted for publication in *IEEE Transactions on Industrial Electronics*, 2015.

©2015 IEEE. Reprinted with permission.

Publication VII

Resonant Test Circuit for High-Power Cascaded Converter Submodules

T. Modeer, S. Norrga, and H.-P. Nee

Published in *Proc. European Conf. Power Electronics and Applications (EPE)*, 2013.

©2013 EPE. Reprinted with permission.

Publication VIII

Implementation and Testing of High-Power IGCT-based Cascaded-Converter Cells

T. Modeer, S. Norrga, and H.-P. Nee

Published in *Proc. Energy Conversion Congress and Exposition (ECCE)*, 2014.

©2014 IEEE. Reprinted with permission.